Astron. Astrophys. 357, 1086–1092 (2000)

ASTRONOMY AND ASTROPHYSICS

Competition of damping mechanisms for the phase-mixed Alfvén waves in the solar corona

Y. Voitenko[1,2] **and M. Goossens**[1]

[1] Centre for Plasma Astrophysics, K.U.Leuven, Belgium (Yuriy.Voitenko@wis.kuleuven.ac.be)
[2] Main Astronomical Observatory, Kyiv, Ukraine

Received 22 November 1999 / Accepted 21 March 2000

Abstract. The competition of the linear and nonlinear damping mechanisms for phase-mixed Alfvén waves in the solar corona is studied. It is shown that the nonlinear damping of the phase-mixed Alfvén waves due to their parametric decay is stronger than both collisional and Landau damping for waves with frequencies below a critical frequency which depends on the wave amplitude. This critical frequency is close to the cyclotron frequency ($\sim 10^5\,\mathrm{s}^{-1}$ in holes) even for small wave amplitudes of the order of 1% of the background value for the magnetic field. This means that the dissipation of the Alfvén wave flux in the corona can be significantly affected by the nonlinear wave dynamics. Nonlinear decay of the low-frequency Alfvén waves transmits a part of the wave energy from the length-scales created by phase mixing to smaller scales, where the waves damp more strongly. However, the direction of the effect can be reversed in the high-frequency domain, $10\,\mathrm{s}^{-1} < \omega < 10^4\,\mathrm{s}^{-1}$, where the decay into counterstreaming waves is strongest, because the wave energy is quickly transferred to larger scales, where the actual dissipation is reduced.

These effects are introduced by the vector nonlinearity which involves waves propagating in the different directions across magnetic field. The effects introduced by the scalar nonlinearity may also become important in phase mixing (Voitenko & Goossens, in preparation).

Key words: Magnetohydrodynamics (MHD) – waves – Sun: corona

1. Introduction

Alfvén waves which have short scales in planes perpendicular to the background magnetic field, are now under intense discussion as a possible agent for heating the solar corona. The development of sufficiently short length-scales in Alfvén waves can be due to phase-mixing, a process first studied in the coronal environment by Heyvaerts & Priest 1983. The linear theory of phase mixing and resonant absorption is well-developed in the framework of the classic one-fluid MHD (Goossens 1994; Ireland & Priest 1997; Hood et al. 1997a,b; Ruderman et al. 1998; De Groof et al. 1998; De Moortel et al. 1999).

In the accompanying paper (Voitenko & Goossens 2000 - Paper I hereafter) we have shown that effects related to the non-zero value of the ion Larmor radius in combination with the finite amplitude of the wave variables can be important for Alfvén waves in the solar corona. In particular we showed that this combination causes the parametric decay of the pump Alfvén wave into two daughter Alfvén waves.

Some effects caused in Alfvén waves by the non-zero value of ion gyroradius are kinetic, and for that reason these waves are often referred to as kinetic Alfvén waves (KAWs). However in Paper I we have shown that the parametric decay of the phase mixed Alfvén wave into daughter Alfvén waves does not require kinetic plasma theory but can be studied with the mathematical model of two-fluid MHD. Hence we do not want to stress the kinetic properties of the Alfvén waves and prefer to use the name "Alfvén waves" (AWs) in what follows. In that respect we also note that in many cases two-fluid-MHD effects are more important in the wave dynamics than kinetic effects, as, for example, resistive dissipation dominates over Landau damping for the low-frequency waves (see Sect. 3).

The problem of phase mixing and resonant absorption becomes more complicated when the finite amplitude of AWs have to be taken into account (Poedts & Goedbloed 1997; Nakariakov et al. 1997). For nonlinear Alfvén waves there is a striking difference between ideal (and resistive) MHD and a two-fluid MHD model that takes into account the effects of the non-zero value of the radius of gyration of the ions - finite ion Larmor radius (FLR). In ideal MHD the three-wave resonant interaction of Alfvén waves does not occur while in a two-fluid MHD model with FLR (and/or electron inertia) the three-wave interaction does exist. As shown in Paper I, this interaction is important for phase-mixing of AWs. As phase mixing of Alfvén waves proceeds, progressively smaller length scales are created, and the combined effects of the finite amplitude and FLR are progressively enhanced leading to strong parametric decay.

Popular excitation mechanisms for coronal AWs are the excitation by photospheric motions (this mechanism can probably generate low-frequency part of the AW spectrum, $\omega \lesssim 1\,\mathrm{s}^{-1}$), and by chromospheric reconnection events. This last excitation mechanism aims to explain the observational evidences of the

Send offprint requests to: Y. Voitenko presence of higher-frequency AWs, $\omega > 1\,\mathrm{s}^{-1}$, in the corona (Tu et al. 1998); it was first proposed by Axford & McKenzie (1992). Depending on the wave frequency in the range of possible frequencies, $10^{-2}\,\mathrm{s}^{-1} \lesssim \omega \lesssim 10^{6}\,\mathrm{s}^{-1}$, the interplay among various linear and nonlinear dissipation mechanisms can be quite different for a phase-mixed AW.

The aim of this article is to investigate the relative importance of the linear and nonlinear dissipation mechanisms for the phase-mixed Alfvén waves depending on the wave parameters and the background plasma.

2. The model

We study the competition of damping mechanisms for phase-mixed Alfvén waves using the WKB-ansatz:

$$A = A_0 \times \exp\left(-i\omega t + i\int \mathbf{k}\cdot d\mathbf{r} + \int \gamma dt\right). \tag{1}$$

The wave vector $\mathbf{k}$ and the growth/damping rate γ obey a local dispersion relation, and integration is along the path of wave propagation. This approximation supplies the description of the waves with parallel wavelengths λ_z and perpendicular wavelengths $\lambda_\perp$ that satisfy the inequalities $\lambda_z < L_\parallel$ and $\lambda_\perp < L_\perp$. $L_\parallel$ and $L_\perp$ are the length-scales of the variations of the equilibrium quantities in the direction along the magnetic field ($\parallel \mathbf{B}_0$) and across the magnetic field ($\perp \mathbf{B}_0$) respectively.

We take the AW eigenmode equation, derived by the use of two-fluid MHD (Paper I), as the basic equation governing both the linear and the nonlinear dynamics of AWs. This equation gives the following expressions for the damping rates of AWs: the collisional damping rate is

$$\gamma_c = -0.25\nu_e \frac{k_\perp^2\delta_e^2}{1+k_\perp^2\delta_e^2}, \tag{2}$$

the damping rate due to (nonlinear) parametric decay,

$$\gamma_{Np} = -0.1\,(p+1)\,\Omega_i \frac{V_A}{V_{Ti}} \varkappa^p \left|\frac{B_k}{B_0}\right|, \tag{3}$$

where $p = 2$ for the decay into counterstreaming waves, and $p = 3$ for the decay into co-streaming wave. The notations are as follows: ν_e is the electron collisional frequency

$$\nu_e = \frac{4\sqrt{2\pi}\Lambda e^4 n_e}{3\sqrt{m_e}T_e^{3/2}}, \tag{4}$$

Λ is the Coulomb logarithm, δ_e is the electron skin length, $\varkappa = k_\perp\rho_i$, $k_\perp$ is the perpendicular wavenumber, ρ_i is the ion gyroradius, V_A and $V_{T\alpha}$ are the Alfvén and the thermal velocities, and B_k is the wave amplitude.

The local dispersion of short-scale AWs is (Paper I)

$$\omega = k_z V_A K\left(k_\perp\right). \tag{5}$$

The function

$$K\left(k_\perp\right) = \left[\frac{1+k_\perp^2\bar\rho_i^2}{1+k_\perp^2\delta_e^2} - \beta\frac{1}{1+k_\perp^2\bar\rho_i^2}\right]^{\frac{1}{2}} \tag{6}$$

is the dispersion function of AWs; it gives the factor by which the parallel phase velocity of the AWs with perpendicular wavelength $2\pi/k_\perp$ exceeds V_A. For an intermediate-β plasma, $m_e/m_i < \beta < 1$, a good approximation for $K^2(\varkappa)$ is

$$K(\varkappa) \approx \left[1 + (1+\frac{T_e}{T_i})\varkappa^2\right]^{\frac{1}{2}}.$$

As this two-fluid AW dispersion relation is close to the kinetic dispersion relation at $\varkappa < 1$ (the kinetic dispersion is $K^2(\varkappa) \approx 1 + (3/4 + T_e/T_i)\varkappa^2$), and since these two dispersion relations are equal for $\varkappa > 1$, we include the kinetic Landau damping in our formulation, taken from the kinetic theory (Voitenko 1998a)

$$\gamma_L = -\sqrt{\frac{\pi}{8}}\omega_k \frac{\varkappa^2}{K}\frac{T_e}{T_i}\frac{V_A}{V_{Te}}. \tag{7}$$

As we have explained in Paper I, the Heyvaerts-Prist-like decay of the wave amplitude with height, $\exp\left(-z^3\right)$, is common for collisional dissipation and nonlinear decay into counterstreaming waves:

$$\begin{aligned} A &= A_0 \times \exp\left(\int \gamma_d \left(\frac{\partial\omega}{\partial k}_z\right)^{-1} dz\right) \\ &= A_0 \times \exp\left(-\frac{z^3}{z_d^3}\right), \end{aligned} \tag{8}$$

where $d = c$ for collisional dissipation, or $d = N2$ for nonlinear damping into counterstreaming waves. The collisional damping distance, z_c, and the distance of the nonlinear decay, z_{N2}, are respectively,

$$z_c = l_\omega \left(\frac{\nu_e}{\Omega_e}\right)^{-\frac{1}{3}}, \tag{9}$$

and

$$z_{N2} = l_\omega \left(\frac{V_{Ti}}{V_A}\left|\frac{B_k}{B_0}\right|\right)^{-\frac{1}{3}}, \tag{10}$$

where the common coefficient

$$l_\omega = \left(0.1\frac{\omega^2}{\Omega_i^2}\frac{\Omega_i}{L_\perp^2 V_A}\right)^{-\frac{1}{3}}. \tag{11}$$

3. Collisional dissipation versus kinetic damping

The aim is to investigate the relative importance of various linear and nonlinear damping mechanisms of AWs depending on their frequency and amplitude. A first logical step in this investigation is to try and figure out which of the linear dissipation mechanisms is the most effective. Here also it is not obvious to give a straightforward answer as it depends on the frequency and on the conditions in the various parts of the solar corona.

Since Landau damping (7) can be important for high-frequency AWs, let us first examine the relative importance of resistive dissipation and Landau damping for the short-scale AWs.

3.1. *The crossover frequency*

The dissipation of an AW due to kinetic electron Landau damping is given by (7). When we take (2) for the dissipation of an AW due to e-i collisions, and compare it with (7), we find that collisional dissipation is stronger, $|\gamma_c| > |\gamma_L|$, for the low-frequency part of the AW spectrum:

$$\omega_k < \omega_{cL}. \tag{12}$$

Here ω_{cL} is the crossover frequency,

$$\omega_{cL} = \frac{K}{1 + k_\perp^2 \delta_e^2} \omega_{cL}^*, \tag{13}$$

with

$$\omega_{cL}^* = \sqrt{\frac{2}{\pi}} \nu \frac{V_A}{V_{Te}}. \tag{14}$$

The crossover frequency ω_{cL} increases with $k_\perp$ until $k_\perp^2 \rho_i^2 = \rho_i^2/\delta_e^2 - 2/(1 + T_e/T_i)$, where it attains its maximal value

$$\omega_{cL\,\max} = \frac{\rho_i}{\delta_e} \sqrt{\frac{1 + T_e/T_i}{4}} \omega_{cL}^*. \tag{15}$$

As $\rho_i \gg \delta_e$ in the corona, then $\omega_{cL\,\max} \gg \omega_{cL}^*$, but this is valid for strong wave dispersion, $k_\perp^2 \rho_i^2 \gg 1$.

It is interesting that in the limit of weak wave dispersion – which is likely to occur for the coronal phase-mixing – the critical frequency does not depend on the wave parameters:

$$\omega_{cL} = \sqrt{\frac{2}{\pi}} \nu \frac{V_A}{V_{Te}}. \tag{16}$$

So we have the same dependence of the damping rate on the perpendicular wavenumber, $\sim k_\perp^2$, for both damping mechanisms for weakly dispersed AWs.

For the waves with frequencies above the critical frequency, $\omega_k > \omega_{cL}$, we find a strong damping of the phase-mixed AWs due to kinetic Landau damping.

3.2. *Estimations of ω_{cL} for coronal holes and active regions*

The damping rate of a phase-mixed AW due to e-i collisions is

$$\gamma_c \simeq -0.25 \nu_e k_\perp^2 \delta_e^2 \tag{17}$$

in coronal holes, where $k_\perp^2 \delta_e^2 \ll k_\perp^2 \rho_i^2 \ll 1$.

The temperatures and densities of electrons in coronal holes are rather well determined (see Wilhelm et al. 1998 and references therein). ν_e may be estimated as $\nu_e \sim 10\,\mathrm{s}^{-1}$ with typical $T_e \lesssim 10^6$ K and $n_e \lesssim 10^8\,\mathrm{cm}^{-3}$ in holes.

Collisional dissipation is stronger than Landau damping if $\omega_k < \omega_{cL}$, where the critical frequency ω_{cL} is given by (13). The critical frequency $\omega_{cL} \simeq 1\,\mathrm{s}^{-1}$ for typical coronal hole conditions, where $V_A/V_{Te} = 1/2$, $\nu = 0.5\nu_e = 4\,\mathrm{s}^{-1}$.

For the active regions we have the estimation $\omega_{cL} = 10$–$100\,\mathrm{s}^{-1}$. Therefore, Landau damping becomes important for much lower frequencies in holes than in active regions, where even relatively high-frequency AWs damp collisionally.

4. Collisional dissipation versus parametric decay

To analyse the competition of the linear and nonlinear damping of the phase-mixed AWs with height in the solar corona, we use the WKB-ansatz (1) for the AW amplitude. We consider here the case of $\omega_k < \omega_{cL}$, when the linear wave damping is dominated by the collisional dissipation.

4.1. *Damping of phase-mixed AWs due to parametric decay instability*

When we use (3) in (8) we find the damping of the wave amplitude with height due to the parametric decay of type $p = 2$ (decay into counterstreaming waves), and due to the decay $p = 3$ (into parallel-propagating waves):

$$A = A_0 \times \exp \sum_{p=2,3} \left(- \frac{z^{p+1}}{z_{Np}^{p+1}} \right),$$

where the nonlinear damping distance of p type is

$$z_{Np} = \left[0.1 \frac{\Omega_i}{V_{Ti}} \left(\frac{\omega}{\Omega_i} \frac{V_{Ti}}{V_A} \frac{1}{L_\perp} \right)^p \left| \frac{B_k}{B_0} \right| \right]^{-\frac{1}{(p+1)}}. \tag{18}$$

The damping due to the $p = 2$ decay is stronger than that due to $p = 3$ decay for the phase-mixed AWs in the corona, where $z_{N2} < z_{N3}$. However, the $p = 2$ decay may be reduced by the parallel nonuniformity in the long-wave domain, $\varkappa^2 < \lambda_z/L_\parallel$ (Paper I).

The restriction on the decay into counterstreaming AWs, placed by the field-aligned plasma nonuniformity, maps onto the frequencies as

$$\omega > \frac{2\pi V_A}{L_\parallel \varkappa^2}. \tag{19}$$

As $\varkappa$ varies with height up to its maximal value determined by the dissipative length-scales, $\varkappa_d = 2\pi\rho_i/\lambda_d$, the decay into counterstreaming waves is important for the waves with frequencies

$$\omega > \frac{V_A \lambda_d^2}{2\pi L_\parallel \rho_i^2}. \tag{20}$$

Since the perpendicular length-scale varies with height as $\lambda_\perp = (\lambda_z/z) L_\perp$, the dissipative length-scale λ_d is related to the dissipation distance z_d through

$$\lambda_d = \frac{\lambda_z}{z_d} L_\perp,$$

and we take $z_d = z_{N2}$. Hence we can to write the condition for the decay into counterstreaming waves as

$$\omega > \omega_2^*,$$

where the marginal frequency

$$\omega_2^* = \frac{V_A}{V_{Ti}} \left[(2\pi)^3 \frac{\rho_i L_\perp^2}{L_\parallel^3} \left[0.1 \left| \frac{B_k}{B_0} \right| \right]^2 \right]^{\frac{1}{5}} \Omega_i.$$

In holes, ω_2^* can vary from $50\,\mathrm{s}^{-1}$ with $L_\perp = 1\,\mathrm{km}$, up to $500\,\mathrm{s}^{-1}$ with $L_\perp = 100\,\mathrm{km}$.

In the case $\omega < \omega_2^*$ we take the $p = 3$ decay as the dominant nonlinear damping mechanism competing with the linear damping mechanisms.

The condition that the nonlinear damping is stronger than the collisional dissipation, $z_{Np} < z_c$, may be written as a threshold condition for the wave amplitude:

$$\left|\frac{B_k}{B_0}\right| > \left|\frac{B_k}{B_0}\right|_{\mathrm{thr}} = (0.1)^{\frac{(p-2)}{3}} \left[\left(\frac{\nu_e}{\Omega_i}\frac{m_e}{m_i}\right)\right]^{\frac{(p+1)}{3}} \times \left(\frac{V_{Ti}}{V_A}\right)^{\frac{1-2p}{3}} \left(\frac{\omega}{\Omega_i}\frac{\rho_i}{L_\perp}\right)^{\frac{2-p}{3}}. \qquad (21)$$

4.2. *The case $p = 3$: decay into parallel-propagating daughter waves*

Although the decay of a pump AW into two parallel-propagating AWs is weaker than the decay into two counterstreaming AWs in a uniform plasma, it can come into play when the field-aligned inhomogeneity depresses the decay into counterstreaming waves. This can happen for the long-scale part of the AW spectrum, $\varkappa^2 < \lambda_z/L_\parallel$, resulting from the phase-mixing of AWs with low frequencies in the regions of the corona with a weak perpendicular inhomogeneity.

The total damping rate is then given by the sum of the collisional decrement and the nonlinear $p = 3$ decrement:

$$\gamma = \gamma_c - \gamma_{N3} = -0.5\nu k_\perp^2 \delta_e^2 - 0.4\Omega_i \frac{V_A}{V_{Ti}} \varkappa^3 \left|\frac{B_k}{B_0}\right|.$$

Taking integrals in the exponent of (1) we find the behaviour of the amplitude with height as

$$A = A_0 \times \exp\left(-\frac{z^3}{z_c^3} - \frac{z^4}{z_{N3}^4}\right), \qquad (22)$$

where the collisional damping distance, z_c, is given by (9), and the nonlinear damping distance is given by (18) with $p = 3$. Since the collisional damping distance, z_c, does not depend on the wave amplitude, it is useful to measure the distances z in units of z_c, $\bar{z} = z/z_c$:

$$A = A_0 \times \exp\left(-\bar{z}^3 - q_{c3}^4 \bar{z}^4\right), \qquad (23)$$

where

$$q_{c3} = \frac{z_c}{z_{N3}}. \qquad (24)$$

The value of parameter q_{c3} determines which process is more efficient, collisional dissipation or parametric decay.

In a coronal hole, where $\nu_e = 10\,\mathrm{s}^{-1}$, $\Omega_i = 9.6 \times 10^4\,\mathrm{s}^{-1}$, $V_{Ti} = 9.1 \times 10^6\,\mathrm{cm\,s}^{-1}$ $V_A = 2.2 \times 10^8\,\mathrm{cm\,s}^{-1}$, the collisional damping height is

$$z_c = 1.8 \times 10^5 \left(\frac{L_\perp(\mathrm{km})}{\omega(\mathrm{s}^{-1})}\right)^{\frac{2}{3}} (\mathrm{km}), \qquad (25)$$

which can be estimated as $z_c = \left(10^2 - 10^3\right) \times \lambda_z$ for the transversal nonuniformity length-scales in the range $L_\perp = (1 - 10^3)\,\mathrm{km}$. The nonlinear damping height of a finite-amplitude ($B/B_0 = 0.03$) AW is

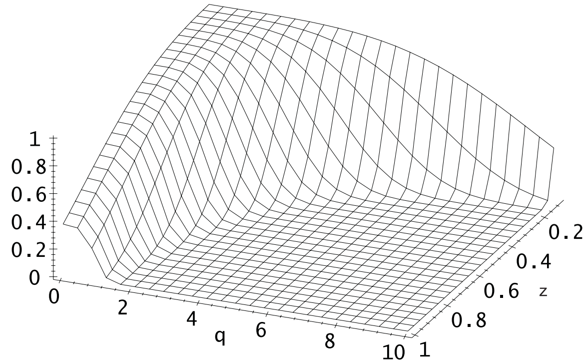

Fig. 1. Damping of the amplitude of the phase-mixed Alfvén wave with the coronal height z for the different values of q, the ratio of the collisional and nonlinear ($p = 3$) damping heights. The wave amplitude is measured in units of the initial amplitude, and the height z in units of the collisional damping height z_c.

$$z_{N3} = 4.5 \times 10^4 \left(\frac{L_\perp(\mathrm{km})}{\omega(\mathrm{s}^{-1})}\right)^{\frac{3}{4}} (\mathrm{km}), \qquad (26)$$

and the parameter q_{c3}, weakly depending on the wave frequency and transversal inhomogeneity:

$$q_{c3} = 4\left(\frac{\omega(\mathrm{s}^{-1})}{L_\perp(\mathrm{km})}\right)^{\frac{1}{12}}. \qquad (27)$$

For $L_\perp$ varying from 1 km (Woo 1996) to 10^3 km (visible plume sizes), we get $q_{c3} = 1.6$–3 for the waves of three-five-minute periods, and $q_{c3} = 7$–12 for the waves in the ion-cyclotron range. These estimations show that the nonlinear decay of AWs in the corona is stronger than the collisional dissipation for all possible wave frequencies.

The interplay of the collisional damping and nonlinear damping in the phase-mixing process is shown on the Fig. 1, where z is measured in units of z_c. The dependence of the damping distance on the relative strengths of the nonlinear and collisional dissipations is manifested through the q -dependence. The wave damping can be very different from that in resistive MHD for $q > 1$. Namely, in the wide range of $q \gtrsim 1.5$, the initial phase-mixed waves are completely damped nonlinearly before they reach the collisional dissipation heights, $\bar{z} = 1$.

As can be seen from (22), the variation of the amplitude with height is initially, near the base of the corona, dominated by collisional dissipation. It is essential here to understand that at heights, which are relatively very low compared to the height where collisional dissipation becomes significant, the phase-mixing changes its character from collisional to nonlinear.

The threshold amplitude of the wave magnetic field for phase-mixing to be dominated by nonlinearity, (21), can be approximated in coronal holes as

$$\left|\frac{B_k}{B_0}\right|_{\mathrm{thr}} = 7 \times 10^{-6} \left[\frac{L_\perp(\mathrm{km})}{\omega(\mathrm{s}^{-1})}\right]^{\frac{1}{3}}. \qquad (28)$$

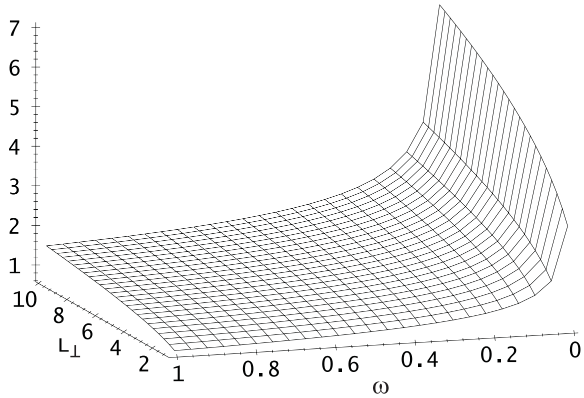

Fig. 2. The threshold wave amplitude (measured in the units of 10^{-5}), with which the nonlinear ($p = 3$) damping of the phase-mixed AW overcomes collisional dissipation. The frequency ω is measured in s^{-1}, and the transversal length-scale of the plasma inhomogeneity $L_\perp$ is measured in km.

This is very small number for a wide range of perpendicular nonuniformities, $1\,\mathrm{km} < L_\perp < 10^3\,\mathrm{km}$, for all frequencies $\omega \geq 10^{-2}\,\mathrm{s}^{-1}$. All threshold values that appear on the Fig. 2 are much lower than the wave amplitude, $B/B_0 \sim 0.01$, likely for the corona.

4.3. *The case $p = 2$: decay into counterstreaming daughter waves*

The competition of the decay into counterstreaming daughter waves with collisional dissipation has been considered in Paper I. Although the behaviour of the amplitude in the $q - z$ space in this case is very similar to that shown on Fig. 1, the dependence of the q-parameter on the wave parameters is different, up-shifting the q-value, which indicates a stronger decay rate.

In coronal holes, we use the following values for the parameters in our formulae: $\nu_e = 8\,\mathrm{s}^{-1}$, $\rho_i = 95\,\mathrm{cm}$, $V_{Ti} = 9.1 \times 10^6\ \mathrm{cm\,s^{-1}}$, $V_A = 2.2 \times 10^8\ \mathrm{cm\,s^{-1}}$, $\Omega_i = 9.6 \times 10^4\ \mathrm{s}^{-1}$. With these values, the nonlinear damping distance (10) can be approximated as

$$z_{N2}(\mathrm{km}) = 1.2 \times 10^4 \left(\frac{L_\perp(\mathrm{km})}{\omega(\mathrm{s}^{-1})}\right)^{\frac{2}{3}}.$$

where $L_\perp(\mathrm{km})$ is $L_\perp$ expressed in kilometers, and $\omega(\mathrm{s}^{-1})$ is ω expressed in s^{-1}. Together with (25) this gives a very high q-coefficient, $q_{cN2} = 15$.

The threshold (21) is now independent of the wave characteristics and the plasma inhomogeneity:

$$\left|\frac{B_k}{B_0}\right|_{\mathrm{thr}} = \frac{V_A}{V_{Ti}}\frac{\nu_e}{\Omega_e}.$$

In coronal holes and in active regions the threshold is almost the same, $|B_k/B_0|_{\mathrm{thr}} \sim 10^{-6}$.

5. Nonlinear decay and Landau damping

In addition to collisional dissipation and nonlinear damping, the high-frequency short-scale AWs undergo also (linear) kinetic Landau damping. The damping rate is given by (7). Therefore, the amplitude of the pump AW changes not only because of collisional/nonlinear dissipation, but also due to collisionless wave-particle interaction. Now we know that the linear damping is dominated by the collisional dissipation in the low-frequency domain, $\omega_k < \omega_{cL}$, and by Landau damping in the high-frequency domain, $\omega_k > \omega_{cL}$. Hence we have to study the relative importance of the nonlinear decay to Landau damping in the high-frequency diapason, $\omega_k > \omega_{cL}$, and of nonlinear decay to collisional dissipation in the low-frequency diapason, $\omega_k < \omega_{cL}$.

In this section we study the damping of a finite-amplitude AW with frequency $\omega_k > \omega_{cL}$, for which the competition between nonlinear damping and Landau damping is important. To describe the dissipation of high-frequency AWs we have, in principle, to use the kinetic plasma model, accounting for the Landau damping. However, we know that the two-fluid MHD dispersion of AWs is close to the exact kinetic dispersion in the whole range of perpendicular wavenumbers and frequencies. Hence we use the two-fluid MHD model with the semi-empirically included Landau damping (7). The Landau damping of the weakly-dispersive AWs is

$$\gamma_L = -\sqrt{\frac{\pi}{8}}\omega_k \frac{T_e}{T_i}\frac{V_A}{V_{Te}}\varkappa^2. \qquad (29)$$

This also leads to a Heyvaerts-Priest behaviour of the wave amplitude, $\sim \exp\left(-z^3/z_d^3\right)$, with the damping distance

$$z_L = l_\omega \left(\sqrt{2\pi}\frac{m_e}{m_i}\frac{V_{Te}}{V_A}\right)^{-\frac{1}{3}} \left(\frac{\omega}{\Omega_i}\right)^{-\frac{1}{3}}. \qquad (30)$$

5.1. *Landau damping versus parametric decay into counterstreaming waves*

In the frequency range $\omega > \omega_2^*$ the decay into counterstreaming waves ($p = 2$) competes with the Landau damping. Taking the damping rate

$$\gamma = \gamma_L - \gamma_{N2} = -0.5\nu k_\perp^2 \delta_e^2 - 0.3\Omega_i \frac{V_A}{V_{Ti}}\varkappa^2 \left|\frac{B_k}{B_0}\right|$$

in (1), we find here the same decay of the wave amplitude with height as in (8), but with the cumulative dissipation distance

$$z_{LN2} = \left(1 + q_{LN2}^3\right)^{-\frac{1}{3}} z_L, \qquad (31)$$

where the Landau damping distance is given by (30) and the q -coefficient is now

$$q_{LN2} = \frac{z_L}{z_{N2}} = \left(\frac{m_i}{2\pi m_e}\frac{T_i}{T_e}\right)^{\frac{1}{6}} \left|\frac{B_k}{B_0}\right|^{\frac{1}{3}} \left(\frac{\omega}{\Omega_i}\right)^{-\frac{1}{3}}.$$

The q-coefficient for a isothermal hydrogen plasma,

$$q_{LN2} = \frac{z_L}{z_{N2}} = 2.6 \left|\frac{B_k}{B_0}\right|^{\frac{1}{3}} \left(\frac{\omega}{\Omega_i}\right)^{-\frac{1}{3}},$$

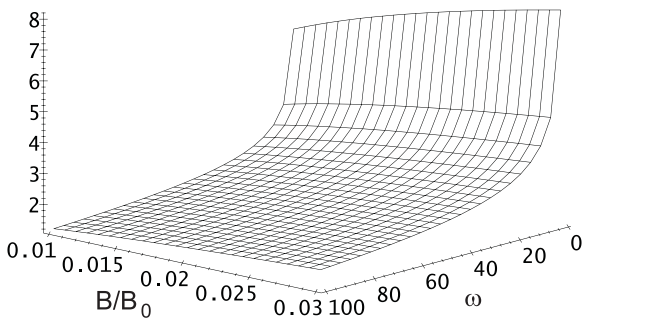

Fig. 3. The relative strength (the q-coefficient) of the $p = 2$ decay and the Landau damping. The frequency ω is measured in units of $10^{-3}\Omega_i$, and B/B_0 is the wave/background magnetic field ratio.

is shown on the Fig. 3. From this figure it is seen that in coronal holes ($\Omega_i = 10^5\,\mathrm{s}^{-1}$), the $p = 2$ decay is stronger than the Landau damping ($q > 1$) for the waves with amplitudes $B/B_0 = 0.1$–0.3 and frequencies $\omega = 10^2$–$10^4\,\mathrm{s}^{-1}$. Only in the vicinity of the cyclotron frequency such waves are damped before they decay into secondary waves.

The nonlinear damping dominates if $q_{LN2} > 1$, and the threshold wave amplitude is

$$\left|\frac{B_k}{B_0}\right|_{\rm thr} = \left(\frac{2\pi m_e T_e}{m_i T_i}\right)^{\frac{1}{2}} \frac{\omega}{\Omega_i} = 6\times10^{-2}\frac{\omega}{\Omega_i}.$$

In this case the threshold amplitude depends on the wave frequency but it does not depend on the plasma inhomogeneity. It is only for frequencies in the ion-cyclotron range this threshold is larger than the assumed AW amplitudes, $B_k/B_0 = 0.03$, and the nonlinear damping looses the competition with Landau damping.

Alternatively, taking the wave amplitude as known, we find the frequencies at which the nonlinear damping dominates:

$$\frac{\omega}{\Omega_i} < \frac{\omega_{LN2}}{\Omega_i} = \left(\frac{2\pi m_e T_e}{m_i T_i}\right)^{-\frac{1}{2}} \left|\frac{B_k}{B_0}\right|. \qquad (32)$$

With the $B_k/B_0 = 0.03$ and $\Omega_i = 10^5\,\mathrm{s}^{-1}$, the values typical for coronal holes, we get $\omega_{LN2} = 5\times10^4\,\mathrm{s}^{-1}$.

In active regions $\omega_{LN2} \sim 10^5$–$10^6\,\mathrm{s}^{-1}$.

5.2. Landau damping versus parametric decay into parallel-propagating waves

Comparing ω_{cL} and ω_2^* we see that usually $\omega_{cL} < \omega_2^*$ in the corona. Then there exists a part of the high-frequency AW spectrum, $\omega_{cL} < \omega < \omega_2^*$, for which the decay $p = 2$ is reduced by the field-aligned inhomogeneity. For these AWs the competition between the $p = 3$ decay and Landau damping may be important. In this case the variation of the amplitude is the same as under the action of collisional dissipation and $p = 3$ decay, but with the q- coefficient

$$q_{LN3} = \frac{z_L}{z_{N3}}. \qquad (33)$$

Taking here (30) for z_L and (21) with $p = 3$ for z_{N3}, we get

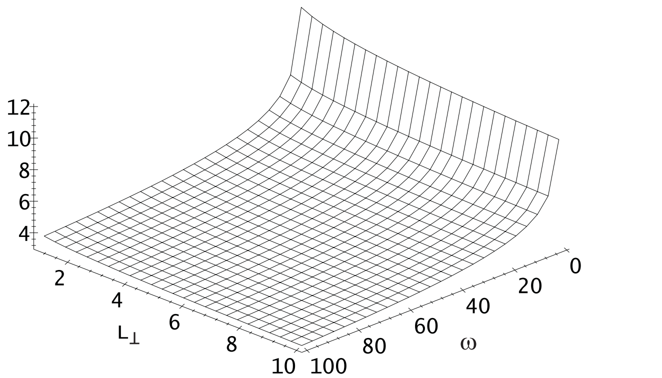

Fig. 4. The relative strength (the q-coefficient) of the parametric ($p = 3$) decay and the Landau damping. The frequency ω is measured in s^{-1}, and the transversal length-scale of the plasma inhomogeneity $L_\perp$ is measured in km.

$$q_{LN3} = \left(\frac{2\pi m_e T_e}{m_i T_i}\right)^{-\frac{1}{6}} \left(10\frac{V_{Ti}}{V_A}\right)^{\frac{1}{12}} \left(\frac{L_\perp}{\rho_i}\right)^{-\frac{1}{12}} \left(\frac{\omega}{\Omega_i}\right)^{-\frac{1}{4}} \left[\left|\frac{B_k}{B_0}\right|\right]^{\frac{1}{4}}. \qquad (34)$$

For the wave amplitudes $B/B_0 = 0.03$ in holes this may be approximated as

$$q_{LN3} = 12\left(\omega^{-\frac{1}{4}}(\mathrm{s}^{-1}) L_\perp^{-\frac{1}{12}}(\mathrm{km})\right), \qquad (35)$$

which is shown on the Fig. 4. It is seen that the ($p = 3$) parametric decay is stronger than the Landau damping in the whole frequency range of interest, $1\,\mathrm{s}^{-1} < \omega < 10^2\,\mathrm{s}^{-1}$.

6. Discussion and conclusions

The effects of the density stratification and magnetic geometry (Ruderman et al. 1998; De Moortel et al. 1999) become important if the wave damping is so slow that the damping distance is comparable to, or exceeds the length-scale of the vertical stratification. To figure out whether these effects are important or not for the nonlinear interaction studied in the present paper, the nonlinear damping distance (18) has to be compared with a characteristic vertical length-scale of the configuration under consideration.

The nonlinear damping of a phase-mixed AW can be due to the excitation of the fast wave at the second harmonic (Nakariakov et al. 1997), but this mechanism requires rather high wave amplitudes, $B/B_0 \gtrsim 0.1$, while the wave amplitudes $B/B_0 \gtrsim 0.01$ are likely for the corona (Saba & Strong 1991; Hara & Ichimoto 1999).

Among the linear dissipation mechanisms of the phase-mixed Alfvén waves in the corona, the collisional dissipation dominates in the frequency range $\omega < \omega_{cL} \sim 1\,\mathrm{s}^{-1}$, and the collisionless Landau damping is dominant in the frequency range $\omega > \omega_{cL} \sim 1\,\mathrm{s}^{-1}$. However with the finite-amplitude ($B/B_0 \gtrsim 0.01$) phase-mixed AWs, the nonlinear interaction is stronger than the linear damping mechanisms in the wide frequency range $\omega < 10^5\,\mathrm{s}^{-1}$. Only the high-frequency part of AW spectrum in the vicinity of the ion-cyclotron frequency is more effectively dissipated by Landau damping (or ion-cyclotron damping at $\omega \sim \Omega_i$).

Namely, the nonlinear decay of the initial AWs into counter-propagating daughter waves dominates in the frequency range $10^2\,\mathrm{s}^{-1} < \omega < 10^5\,\mathrm{s}^{-1}$, while the decay into parallel-propagating daughter waves dominates in the frequency range $\omega < 10^2\,\mathrm{s}^{-1}$.

The resulting ordering of the characteristic frequencies is as follows:

$$\begin{aligned} \omega_{\min}\left(\sim 10^{-2}\mathrm{s}^{-1}\right) &< \omega_{cL}\left(\sim 1\mathrm{s}^{-1}\right) \\ &< \nu_e\left(\sim 10 - 10^2\mathrm{s}^{-1}\right) \\ &< \omega_2^*\left(\sim 10^2\text{–}10^3\mathrm{s}^{-1}\right) \\ &< \omega_{LN}\left(\sim 10^5\text{–}10^6\mathrm{s}^{-1}\right) \\ &\lesssim \Omega_i. \end{aligned}$$

The first number in the parenthesis refers to the coronal hole conditions, and the second – to the active region conditions.

The actual dynamics of the phase-mixed AWs depends on the frequency range where the energy of the waves is concentrated. The spectral redistribution of the wave energy towards larger length-scales, as well as the partial reflection of the wave flux, reduces the rate of the dissipation of the wave flux in the frequency range $10^2\,\mathrm{s}^{-1} < \omega < 10^5\,\mathrm{s}^{-1}$. On the other hand, the dissipation of the low-frequency part of AW spectrum can be accelerated by the decay into parallel-propagating waves, when a part of the wave energy is transported into smaller scales.

Our results show that the nonlinear interaction has important consequences for observing Alfvén waves in the solar corona. In particular, it exclude the possible observation of low-frequency Alfvénic motions in the vicinity of heated regions by the measurements of Doppler shifts of spectral lines. The phase-mixing itself produces short length-scales in the direction of the non-uniformity only. However, the nonlinear interaction spreads out an initial disturbance into a wide spectrum of uncorrelated length-scales in all directions. This excludes the possibility for AWs to be observed at heights $z > z_N$ in the corona by the Doppler shifts, irrespectively of the space and time resolution abilities of a telescope.

The remaining possibility is to observe the flux of Alfvén waves via spectral lines broadening, in which case the broadening in the perpendicular direction, induced by the fluctuations of the perpendicular ion velocity in the wave fields, should be much wider than the parallel broadening induced by the much smaller field-aligned ion velocity in AWs.

It is quite possible that a turbulent state can develop before the wave flux is dissipated, in which case we have to examine the direction of the turbulent cascade, having a strong influence on the eventual dissipation of the wave flux. There are indications that an inverse turbulent cascade is set up by the turbulence of short-scale AWs (Voitenko 1998b), transporting the energy to larger scales and thus reducing the actual dissipation of the AW flux. However, this result has been obtained in the model of dominant triads in the cascading process, induced by the vector nonlinearity, $\sim [\mathbf{k}_1 \times \mathbf{k}_2]_z$ ($\mathbf{k}_1$ and $\mathbf{k}_2$ are the wave vectors of interacting AWs). It has to be verified by a more rigorous analytical and numerical investigation taking into account the scalar nonlinearity, $\sim \mathbf{k}_1 \cdot \mathbf{k}_2$, that may be important in phase mixing (Voitenko & Goossens, in preparation).

There are another, kinetic dissipation mechanisms – (linear) ion cyclotron damping, and (nonlinear) induced ion scattering – which may become important in the phase-mixing. The presence of the AWs with different perpendicular wavelengths (and therefore with different parallel velocities) in the same spatial domain (the result of nonlinear decay), introduces also nonlinear ion Landau damping.

Acknowledgements. This work was supported by the FWO-Vlaanderen grant G.0335.98 and by Intas grant 96-530.

References

Axford W.I., McKenzie J.F., 1992, In: Marsch E., Schwenn R. (eds.) Solar Wind Seven. Pergamon Press, Oxford, England, p. 1
De Groof A., Tirry W., Goossens M., 1998, A&A 335, 329
De Moortel I., Hood A.W., Ireland J., Arber T.D., 1999, A&A 346, 641
Goossens M., 1994, Space Sci. Rev. 68, 51
Hara H., Ichimoto K., 1999, ApJ 513, 969
Heyvaerts J., Priest E.R., 1983, A&A 117, 220
Hood A.W., Ireland J., Priest E.R., 1997a, A&A 318, 957
Hood A.W., Gonzalez-Delgado D., Ireland J., 1997b, A&A 324, 11
Ireland J., Priest E.R., 1997, Solar Phys. 173, 31
Nakariakov V. M., Roberts B., Muravski K., 1997, Solar Phys. 175, 93
Poedts S., Goedbloed J.P., 1997, A&A 321, 935
Ruderman M.S., Nakariakov V.M., Roberts B., 1998, A&A 338, 1118
Saba J.L.R., Strong K.T., 1991, ApJ 375, 789
Tu C.-Y., Marsch E., Wilhelm K., Curdt W., 1998, ApJ 503, 475
Voitenko Yu.M., 1998a, Solar Phys. 182, 411
Voitenko Yu.M., 1998b, J. Plasma Phys. 60, 515
Voitenko Yu.M., Goossens M., 2000, A&A, accepted (Paper I)
Wilhelm K., Marsch E., Dwivedi B.N., et al., 1998, ApJ 500, 1023
Woo R., 1996, Nat 379, 321